ADA284176

REPORT DOCUMENTATION PAGE

Form Approved
OMB No. 0704-0188

1. AGENCY USE ONLY (Leave blank)	2. REPORT DATE August 1994	3. REPORT TYPE AND DATES COVERED Final, June 1992–August 1993

4. TITLE AND SUBTITLE Radiation-Induced Noise in UMPC-Type Current Probes: IEMP Response of the Current Measurement System	5. FUNDING NUMBERS PE: 63215C

6. AUTHOR(S)

James C. Blackburn

7. PERFORMING ORGANIZATION NAME(S) AND ADDRESS(ES) U.S. Army Research Laboratory Attn: AMSRL-WT-NG 2800 Powder Mill Road Adelphi, MD 20783-1197	8. PERFORMING ORGANIZATION REPORT NUMBER ARL-TR-366

9. SPONSORING/MONITORING AGENCY NAME(S) AND ADDRESS(ES) Army Space and Strategic Defense Command PO Box 1500 Huntsville, AL 35807-3801	10. SPONSORING/MONITORING AGENCY REPORT NUMBER

11. SUPPLEMENTARY NOTES

AMS code: 623215.15C1
ARL Pr No.: 328628

12a. DISTRIBUTION/AVAILABILITY STATEMENT Approved for public release; distribution unlimited.	12b. DISTRIBUTION CODE

13. ABSTRACT *(Maximum 200 words)*

The purpose of these tests was to determine the radiation-induced noise response of the probes in fluences up to the maximum obtainable from our high-intensity flash x-ray (HIFX), somewhat above 2×10^{11} rads(Si)/s. This noise level determines the signal-to-noise ratio that can be obtained in low-level current measurements in the pulsed radiation environment, such as input photocurrents to silicon-on-sapphire devices. The UMPC probes themselves are a significant issue because they are at present the most satisfactory way of measuring currents in pulsed radiation; in spite of their limitations a better means is not available.

Not only is the internal electromagentic pulse (IEMP) response of the probe itself presented, but also that of unavoidably related structures is addressed, such as the circuit conductors connecting to the probes. It is found that these connections typically are the limiting factor in determining the measurement system noise level. The lowest noise level attained, about 2.5 mA at 3×10^{11}, was with a two-core transformer.

(continued on reverse)

14. SUBJECT TERMS Current probe; IEMP; radiation-induced noise		15. NUMBER OF PAGES 43
		16. PRICE CODE

17. SECURITY CLASSIFICATION OF REPORT Unclassified	18. SECURITY CLASSIFICATION OF THIS PAGE Unclassified	19. SECURITY CLASSIFICATION OF ABSTRACT Unclassified	20. LIMITATION OF ABSTRACT UL

13. Abstrac ...d)

Operation of the probe in a high-dose-rate environment is essential because it is typically not possible to isolate the probes from the radiation. Attempts to distance the probes from the point of measurement introduce unrealistic stray inductance and capacitance into the system being tested, important at high frequencies (short risetimes) where conductor lengths are kept to a minimum. Often even more significant is the distortion produced by the introduction of the additional IEMP drive intercepted by the added length of conductor. Attempts to "spot shield" small areas (containing probes) are usually unrealistic because radiation sources are extended and produce a sizeable penumbral region of distorted dose rate around small shielding obstacles.

Accesion For		
NTIS CRA&I	☑	
DTIC TAB	☐	
Unannounced	☐	
Justification		
By		
Distribution /		
Availability Codes		
Dist	Avail and / or Special	
A-1		

Contents

Figures

Figures (cont'd)

Tables

4

1. Introduction

This report describes the experimental procedures and results for a series of flash x-ray tests of Jaycor ultra-miniature pulsed current probe transformers (UMPCs). The purpose of the tests was to determine the radiation-induced noise response of the transformers in fluences up to the maximum obtainable from our high-intensity flash x-ray (HIFX), somewhat above 2×10^{11} rads(Si)/s [1]. This is an important parameter, since to be most useful these transformers must have the lowest possible noise response, allowing them to be used to accurately monitor small currents, such as input photocurrents to silicon-on-sapphire (SOS) logic devices, while the device and the probe are both exposed to a high fluence. The transformer must operate in this fluence because in general it is not possible to separate the current probe physically from the device monitored by it; the inductance added by a significant length of conductor would alter circuit response. Also, the added conductor would itself be subject to collecting noise induced by internal electromagnetic pulse (IEMP) currents.

Transformers using a variety of construction techniques were evaluated and compared, as were factors ancillary to their use, such as noise pickup by the printed circuit (PC) board on which the transformer were mounted.

The radiation-induced noise response of the boards was found to be a determining factor in the overall performance of the transformer, and much of the report is therefore devoted to board responses, which were often not in even qualitative agreement with expectations based on accepted IEMP drive mechanisms.

The UMPCs were tested in three groups, spread over about eight months. The first tests showed that the first lot of UMPC transformers had much greater than expected noise response and (as will be shown) suggested problem areas to be overcome. The second series of tests, on a new lot of UMPCs that were prepared so as to highlight the effects of potting materials and the transformer assembly, showed considerable improvement, enough so that the IEMP noise coupled into the test circuit board became suspect as a significant contributor to system noise. This possibility was evaluated in both test-series 2 and 3. The third series of tests used lead collimating apertures to confine the area of radiation and aid in separating transformer responses from those of the circuit board to which the transformers were attached.

2. Description of Current Probes

The Jaycor UMPC is a very small balanced pass-through current transformer similar to its larger predecessor, the MPC-8 [2]. Its concept of operation is the same as that of the well-known Tektronix CT-1 and CT-2 current transformers, but in the UMPC devices a balanced winding, combined with small physical size (small area for collection of IEMP currents) and careful dielectric potting, yields a much reduced response to pulsed radiation. It is intended to be used as a minimally perturbing current monitor, small enough (0.165 × 0.090 × 0.060 in.) to allow it to be inserted directly into circuit boards, where it becomes part of the structure. This requires little modification of the circuit board and thus the added inductance and capacitance are small, allowing nearly undisturbed normal operation of the circuit.

The UMPC (shown in cross section in fig. 1) has a balanced construction, using 12 turns of bifilar-wound 0.001-in. copper wire as the secondary for the transformer, wrapped around a 0.033-in. O.D. Ceramic Magnetics CN20 ferrite core (0.014-in.-thick, 0.011-in.-wide hole). A 50-Ω chip resistor across the secondary reduces the impedance seen by the transformer, increasing the inductance to resistance (L/R) ratio, and thereby decreasing the low-frequency limit. The output signal is transmitted by a balanced transmission line to a balun, which inverts the negative signal and adds it to the positive signal, producing about 0.5 mV of sensor output per mA of primary current (after a 2.5× amplitude reduction due to the balun). The action of the balun rejects common-mode noise drive to the balanced line connecting the transformer to instruments.

Figure 1. Three views of UMPC current probe assembled into ceramic carrier. Thermistor was not included in tested units. The "Ground" connection is typically left floating.

Top view

Side view

Contact side view

6
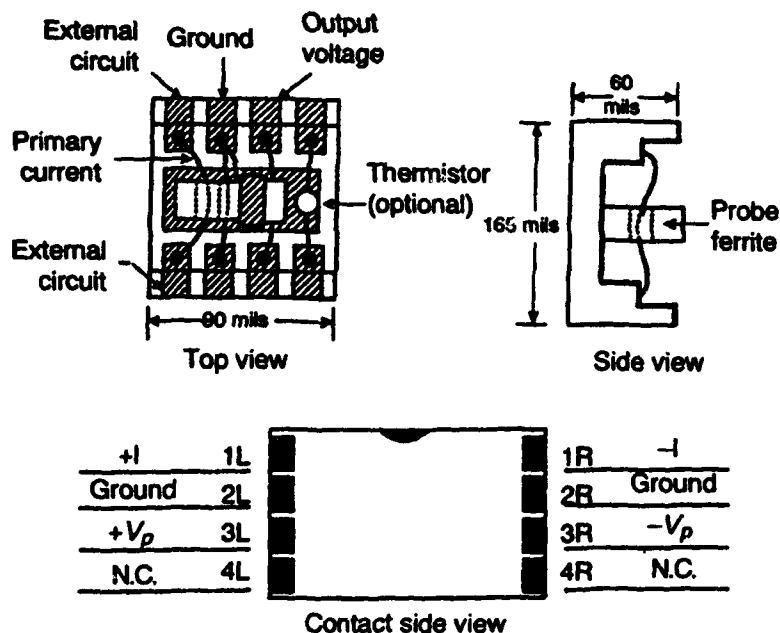
The frequency response of the transformer is nearly flat to above 300 MHz, as shown in figure 2; the associated pulse risetime is about 1 ns. Tests made with pulses showed linear response to above a 15-A peak, with a saturation product of about 300 A-ns.

The UMPC is sufficiently small that it is compatible with high-density interconnect packaging. The carrier shown in figure 1 has 0.015-in.[2] gold bond pads that can be bonded-out with fly wires to pads on a circuit board. Figure 3 illustrates the method used to inte-

Figure 2. Swept-frequency response of transformer.

Start = 50 kHz
End = 500 MHz
−3 dB point = 435 kHz
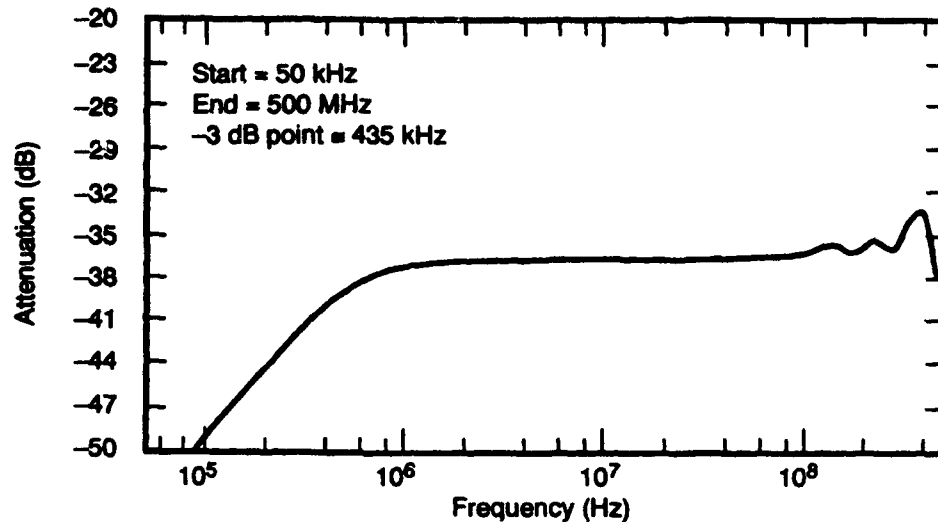
Figure 3. Installation of UMPC transformer into multi-layer circuit board for test-series 1.

Cu lid, attaches to solder frame

100 mils

340 mils I.D.

Top ground

I probe carrier

Surface pads

Ferrite

Lid solder frame

60 mils

Via connecting surface pads to buried trace

Epoxy

Bottom ground and probe attach pad (connects to bottom ground)

Vias connecting grounds

Bottom ground

7
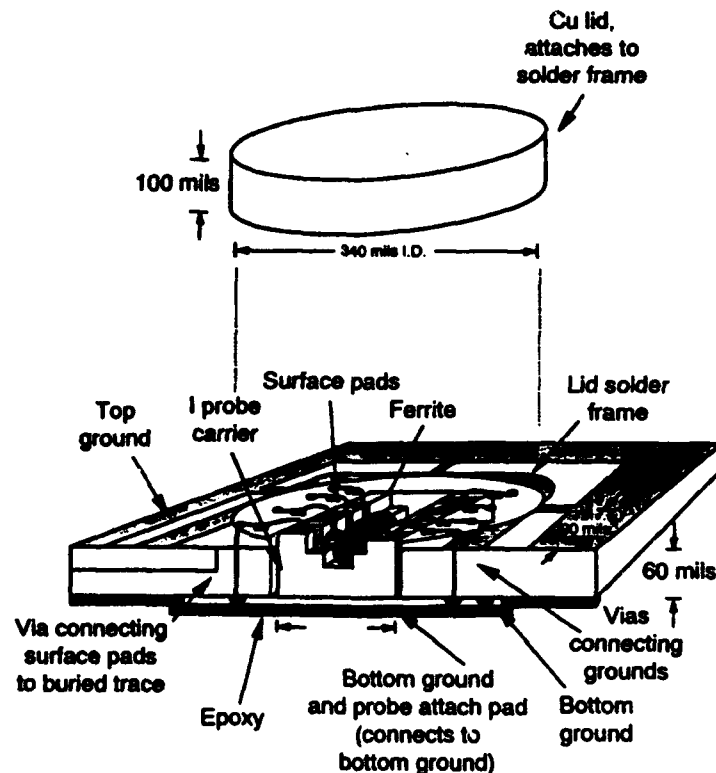
grate the UMPC into the circuit board for the first series of tests. The UMPC fits into a hole cut into the circuit board and attaches to surface pads on the board via aluminum bond wires. The surface pads lead to through-holes which connect to buried signal traces. The probe is epoxied onto a grounded bottom plate that is soldered onto the board ground plane. The internal region, in particular the bond wires, is then covered with HIPEC and a metal cap is soldered onto the board ground plane to complete the shielding enclosure. Around the perimeter of this ring are six through-holes (not shown) that connect the top and bottom ground-planes, stitching an rf barrier around the UMPC. This method of installation into the board became suspect and a second method, shown later in figure 8, in which the flywires between carrier and board are connected to pads emerging from a step cut at the buried signal layer, was used for the second and third test series. This avoided the need for surface pads and through-holes, resulting in less conductor area and consequently a smaller radiation response.

3. Radiation Testing

3.1 Circuit Board

For the first test series the transformers were attached to a circular circuit board, depicted in figure 4, which formed the interface between the transformers and the low-noise test fixture developed by Jaycor [3]. Each board was fitted with four transformers, represented by the small rectangles near the center. Each transformer is connected to the board as shown in figure 3, with the output leads ultimately connected to the test fixture probes by the circular pads at

Figure 4. Current transformers on test board for test-series 1. One transformer, D, is connected by 5-mil traces on the inner layer of the circuit board; other transformers are connected by the standard 10-mil traces.
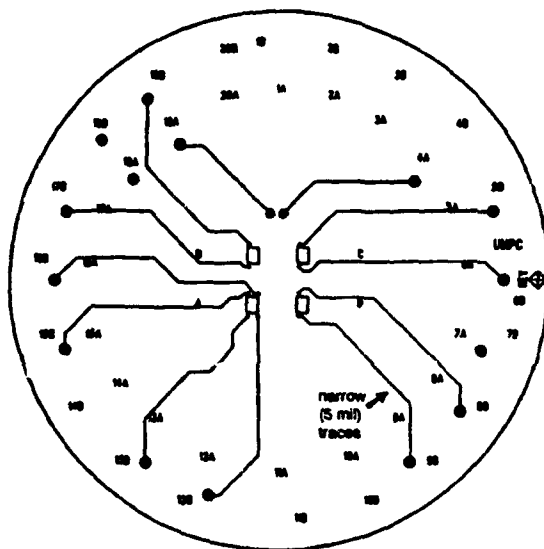
the periphery of the board (numbered 5B, 6B, 8B, 9B, etc). The board itself has ground planes on both sides, and narrow traces, symmetrically placed between the ground planes, connect the signals. This type of construction has a very low radiation-induced noise level [4] because it incorporates narrow traces (with less area for electron collection/emission), symmetrical construction (such that radiation incident normal to the board knocks about as many electrons between first ground plane and trace as between trace and second ground plane, roughly canceling), and polyimide dielectric (which has a low value of radiation-induced conductivity).

3.2   Instrumentation

The instrumentation connected to the board is shown in figure 5. The board is the rectangle indicated by the dotted lines with the numbered circles (5B, 6B, etc) representing the connections to the spring-loaded probes, known as Pogos, which are part of the low-noise test fixture. Two of the Pogos, those connected to 16B and 12B, contain internal current transformers; the remainder of the Pogos are only electrical extensions of the 50-Ω lines. These transformerless Pogo probes have very low noise pickup, less than 1 mV (into 50 Ω) at full fluence, when connected to outer-ring (B) terminals.

Since the UMPC current transformers produce differential signals, it is necessary that the lines connecting to them, including the traces on the board, the Pogo probes, and the cujacs leading to instrumentation, be matched in electrical length. In these tests the match was within a few millimeters. On the board, where radiation is intense, it is also necessary to keep the lines close together so that they experience the same radiation environment, and therefore the same IEMP noise-drive. This is accomplished by the conductor layout of figure 4.

Figure 5. Instrumentation connected to circuit board for test-series 1. Note that two Pogos, connected to 12B and 16B, have integral current transformers.

9
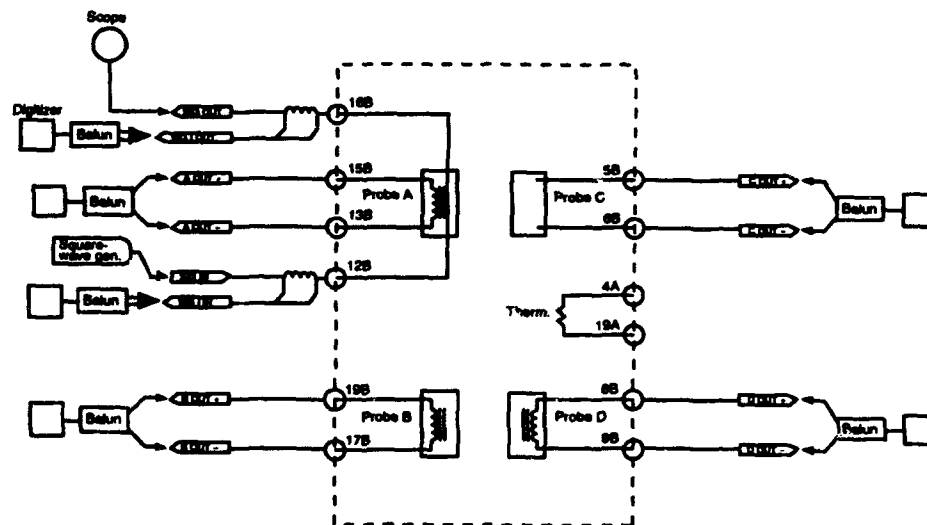
Two different trace widths (5 and 10 mil) are used in connecting the transformers in an attempt to determine the effect of this parameter on noise response. As indicated on figure 4, transformer probes A, B, and C have the wide interconnect traces and probe D the narrow traces. Transformers C and D are nominally identical except for the trace widths.

Transformer "A" has a test signal applied to it, a 10-MHz squarewave. The other end of the line carrying the 10-MHz signal is terminated by an oscilloscope with a 7A29 plug-in. This provides a good 50-Ω termination as well as providing the amplitude reference for the signal. Other probes have no conductor through them; no signal is applied—their output is solely noise.

3.3 Dosimetry

The dosimetry was accomplished by the accepted methods associated with the HIFX: for each shot a foil-wrapped package of three dosimeters was placed on the vacuum-sealing Mylar diaphragm at the end of the low noise test fixture. This placed the dosimeters only a few thousandths of an inch (the Mylar and foil thickness) from the surface of the board on which the transformers were mounted. Calculations by Ovrebo [5], as well as experiments by Smith [6], show that electronic equilibrium is established here by the aluminum and carbon at the HIFX faceplate. The latter (the experiments) showed that the thermoluminescent dosimeters (TLD's) indicated equal dose whether placed in thick aluminum pill boxes or wrapped only in foil.

3.4 Test Procedure

The experiment shot procedure consisted of first allowing the temperature to stabilize at the desired value, then adjusting the squarewave signal to the desired amplitude, placing the desired distance between the test fixture and HIFX so as to obtain (nominally) either 1×10^{11} or 4×10^{11} rads(Si)/s and firing HIFX. All data were then automatically recorded on the digitizers. No effort was made to synchronize radiation with a specific point on the squarewave; this was felt to be unnecessary. No lead collimator was used for the first and second test series; the entire surface of the testboard was exposed.

The signal continuity was checked for all transformers when the test boards were installed, and from time to time during the testing. This was felt to be necessary because in previous work we had observed a slight tendency for the Pogo-to-board contact to loosen, especially

at low temperatures, where lubricants become thickened. We checked for continuity by removing one lead of the balanced line pair from the balun and connecting it to a signal generator, then observing the signal delivered by the other lead of the pair (still connected to balun and digitizer). In all tests, the correct response was observed—a reversal of signal polarity and reduction of amplitude of about one-half.

4. First Test Series

4.1 General Discussion

The shot matrix, table 1, presents an overall view of test conditions and the corresponding shot numbers. Typical high-dose-rate (~4 × 10^{11}) shot results are shown by figure 6, which presents the responses observed in the current transformers on test board number two at 25°C. In examining figure 6, consider first 6(f) (the XRD radiation detector) and 6(e) (the noise output of transformer C). Note that there is a time delay between the peaks of the two signals—that is a result of the approximately 10-ns propagation delay in the balun and its cable. The XRD signal does not pass through a balun, whereas all other signals do and are thereby delayed.

Next consider figures 6(a) and 6(c), the signals from the current transformers in the Pogos connecting the input 10-MHz squarewave to transformer A. These two signals are 180° out of phase, as they should be. The sense of the current, which is supplied from outside

Table 1. Shot matrix of test-series 1.

Test	Temp. (°C)	Input current (mA)	Input freq. (MHz)	Nominal dose rate (Rads/s)	Shot No.				
1	25	5	10	5×10^{10}	5968	5975	—	—	—
2	25	5	10	2×10^{11}	5966	5967	5969	5984	5985
3	25	50	10	5×10^{10}	5972	5987	—	—	—
4	25	50	10	2×10^{11}	5970	5971	5980	5986	—
5	25	100	10	5×10^{10}	5974	—	—	—	—
6	25	100	10	2×10^{11}	5973	—	—	—	—
12	–55	5	10	2×10^{11}	5976	5977	5988	5989	—
14	–55	50	10	2×10^{11}	5979	—	—	—	—
16	–55	100	10	2×10^{11}	5978	5990	—	—	—
22	125	5	10	2×10^{11}	5983	5992	—	—	—
24	125	50	10	2×10^{11}	5981	—	—	—	—
26	125	100	10	2×10^{11}	5982	5991	—	—	—
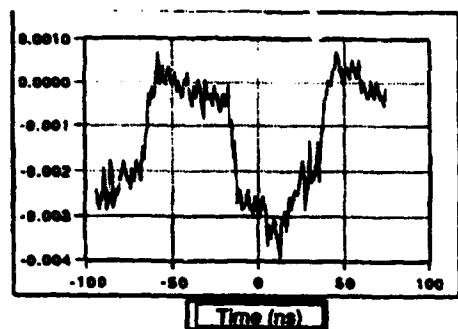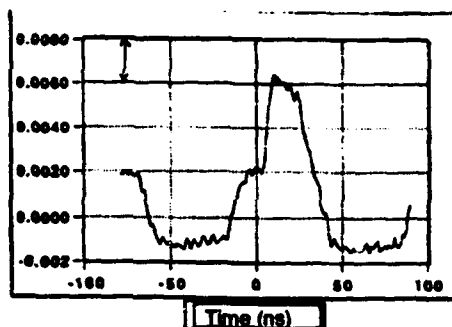
11
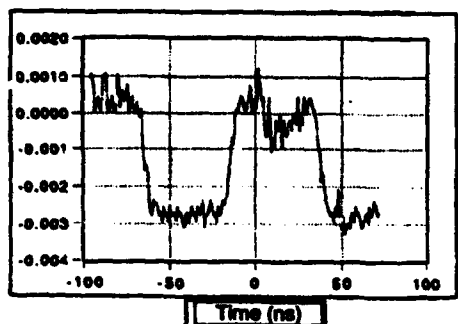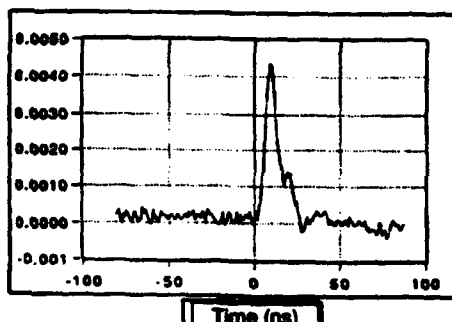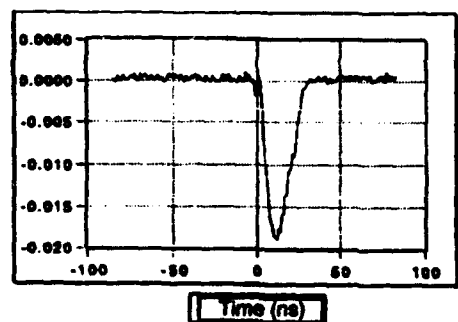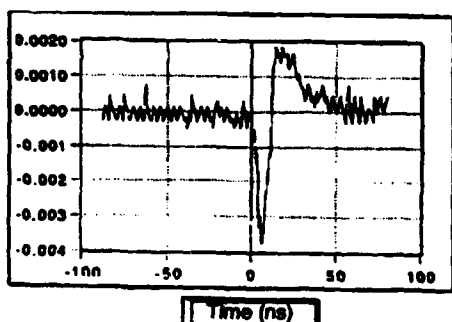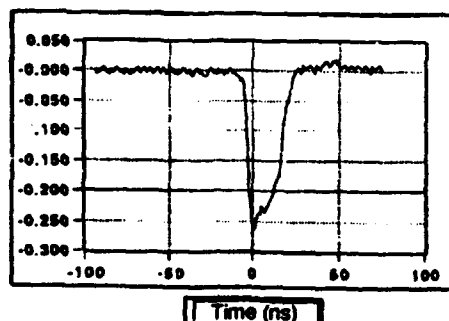
Figure 6. Radiation-induced noise responses of UMPC transformers in test-series 1. Transformer "A" has an externally generated 5-mA squarewave signal applied to it; its response (7b) is therefore the sum of the squarewave and the radiation-induced noise. Radiation level approximately 4×10^{11} at location of transformers (center of board). Temperature, 25°C.

12

the VTS board, is opposite in the two Pogos. At radiation time, about 10 ns, both signals show an excursion of about 1 mV in the same direction; this is also as it should be—the current producing this excursion is incident on the circuit board traces within the VTS board and consequently flows in the same sense through both Pogos. The roughly 1-mV signal corresponds to about a 2-mA radiation-induced current. The total radiation-induced current into the structures on the VTS board is therefore about 4 mA, half flowing through each Pogo connection. Inasmuch as the transformer is very small, with little surface area to receive IEMP drive, and electrostatically well-shielded, it is reasonable to assume that most of this current is induced into the traces on the VTS circuit board, and not into the transformer. It will be seen that this assumption is in reasonable agreement with the measurements on traces, reported later in sections 5.4 and 6.3.

Figure 6(b) shows initially a 3-mV squarewave from transformer A, corresponding to the external current drive applied from the squarewave generator. At $t = 10$ ns, the time of the peak of the radiation pulse, the waveform is driven positive by about 4 mV, corresponding to 8 mA of radiation-induced noise; in the absence of this noise the top of the waveform would have continued level at its value as of 0 ns, just before radiation.

Note that the above-mentioned 4-mA radiation drive to the traces should be expected to contribute little to this noise signal: the physical symmetry of the board is such that, as viewed from the transformer, equal current contributions should enter both traces and thus cancel at the balun transformer.

Figure 6(d) shows a similar noise response, about 4 mV (8 mA), for transformer B. The noise response is easy to discern here since no squarewave is superimposed on it. Although the shape of the noise current is different from that in figure 7(b), the full-width durations are approximately equal to the full width of the HIFX pulse—about 30 ns.

Figures 6(e) and 6(f) are the noise outputs of transformers C and D. The reason for the considerable increase in amplitude of the noise from transformer C (it peaks at –18 mV, –40 mA) is not evident, although it is likely due to incomplete dielectric insulation on signal-carrying conductors.

The peak noise response of transformer D, about 3 mV (6 mA), is the least of the four; this may be related to the fact that the traces connecting it to the Pogos are thinner (5 mils) than those of the other transformers. The reason for the bipolar signal is not evident, although, as will be seen in the following shot, it is not a unique response.

13

Figure 7 shows corresponding traces for shot 5977, where the above transformers were irradiated while at –55°C. The dose rate was about 80 percent of that of the preceding room-temperature shot.

The response of transformer A is similar in shape to that at room temperature, although about 2.5 times as great, considering the reduced dose rate. Transformer B now has a bipolar response and its return to zero level is delayed. Transformers C and D have surprising responses, with extremely delayed returns to zero.

Similar disparities were observed between the +25°C and –55°C responses of the transformers on VTS board number 1, although the maximum noise duration (at –55°C) was not as great as for board number 2 (described above).

Testing was at this point discontinued (shot 5992), both because the alloted HIFX time had run out and because it was obvious that these transformers were not satisfactory. Section 4.2 summarizes the results of this first series of tests, and the following sections describe further tests (series 2 and 3) on new VTS boards with improved transformers.

4.2 Results and Discussion

Table 2 attempts to summarize all results, although it is not possible with a few numerical entries to fully describe some of the more unusual waveforms. The order of the entries—probe B, C, D, and A—is chosen in order to group together probes B and C, which are nominally identical, and then present the next probe, D (which has 5-mil interconnects, not 10 mil) and then finally probe A, which is unique in that it has a test waveform applied.

It is quite conspicuous in the table that transformer C on board number 2 has a problem with temperature extremes, expecially low temperatures. At –55°C, its noise response is much greater in amplitude than at room temperature, and the asterisks indicate that the duration of the response is long—much longer than the total duration of the radiation pulse. The same strongly increased amplitude response, but without the extreme duration, occurred at +125°C. No systematic difference seems to have been produced by the use of 5-mil board traces to transformer D; it does not, on the average, have a response different from B or A, which use 10-mil traces for connections.

It is probable that some kind of physical distortion, produced by differential thermal expansion coefficients, caused the extreme noise responses at low temperatures. It should be noted that the problem
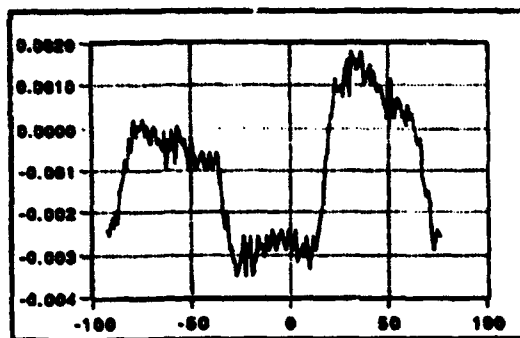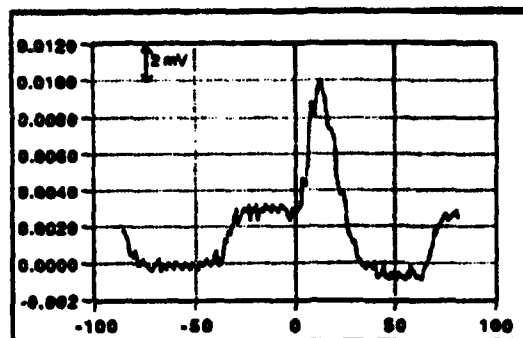
14
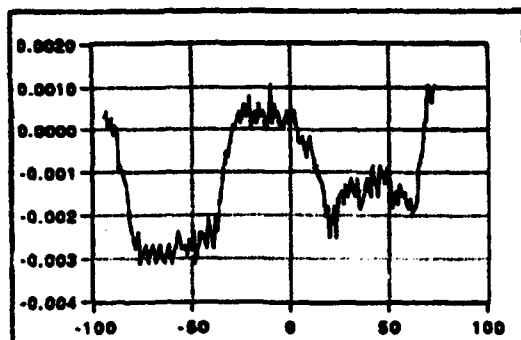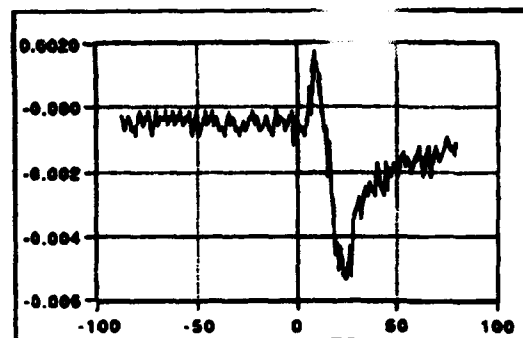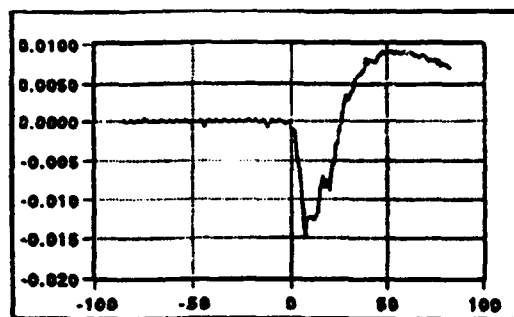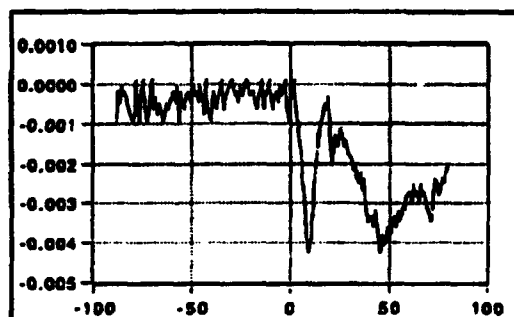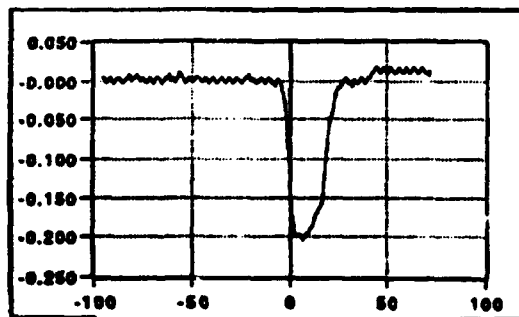
Figure 7. Radiation-induced responses of UMPC transformers to radiation in test-series 1. As in figure 6, except temperature here –55°C. A stretched response is evident in B, C, and D.

Table 2. Summary of results, test-series 2.

Shot	Board No.	Temp (°C)	Dose (krads (Si))	Squarewave current (mA)	Peak noise output (mV) (Current = mV × 2.4) Probe: B	C	D	A
5966	1	+25	3.5 Hi	5	−2.8	−5.5	+4	2
5967	1	+25	4.7 Hi	5	−3.0	−9	+6	4
5968	1	+25	1.3 Lo	5	+1.5	−3.0	<1	2
5969	2	+25	4.5 Hi	5	+4.5	−1.8	−3.8	4
5970	2	+25	4.6 Hi	50	+3.0	−1.8	−4.0	8
5971	2	+25	4.1 Hi	50	+3.7	−1.7	−3.8	7
5972	2	+25	1.1 Lo	50	?	−6.0	−3.0	5
5973	2	+25	4.6 Hi	100	+5.5	−20.	±3.5	10
5974	2	+25	1.1 Lo	100	+4.5	−8	−2.5	?
5975	2	+25	1.2 Lo	5	+4	−7	−1	5
5976	2	−55	3.8 Hi	5	−6	−15*	−2.5*	8
5977	2	−55	3.3 Hi	5	−5	−15*	−4*	8
5978	2	−55	3.9 Hi	100	−6	±15*	−4*	6
5979	2	−55	3.4 Hi	50	−5.5	±12*	−4	7
5980	2	+25	3.3 Hi	50	+3.0	−17	+8	6
5981	2	+125	3.3 Hi	50	+2.0	−25	+1.5	?
5982	2	+125	3.6 Hi	100	+4	−22	+1.5	?
5983	2	+125	3.3 Hi	5	+4	−21	+1	4
5984	1	+25	2.6 Hi	5	+4	+7	±1	2.5
5985	1	+25	3.8 Hi	5	−2	−4	+5.5	2
5986	1	+25	3.7 Hi	50	−3.5	−4	+6	3
5987	1	+25	1.0 Lo	50	<1	−2.5	+0.5	?
5988	1	−55	3.9 Hi	5	−13	>+10	+10	4
5989	1	−55	4.1 Hi	5	−14	+14	+10	3
5990	1	−55	3.7 Hi	100	−14	+15	+8	?
5991	1	+125	3.8 Hi	100	+1.5	−3	+2	?
5992	1	+125	3.7 Hi	5	+2	±2	+4	2

*Indicates that noise signal is of greater duration than radiation.

was not a break in the leads coming from the transformer: a transmitted-pulse test, described in section 3.4, was applied immediately after all radiation tests where unusual responses were seen and no failures were observed at any time.

Unfortunately, even at favorable temperatures the noise response is stronger than desired—the response at the high dose rate being about 3 or 4 mV (7 to 9 mA) at room temperature. This is a smaller response than the average seen in the original MPC-8 transformer [2], but is not quite as good as the least-noisy of these transformers.

It is thought that this high noise level may be a result of the Hipec flowing away from its desired location during the heating required to solder the transformer lid (fig. 3) to the circuit board [7].

5. Second Test Series

5.1 General Discussion

The first series of tests on UMPC transformers indicated generally higher-than-expected noise levels, and at low temperature (−55°C) a long recovery persisted in the noise response. These responses were presumed to be a result of potting materials separating from conductors, allowing IEMP from knock-off electrons to be collected. For this reason, a new method was designed for attaching the transformers to the test board, and several changes were made in the UMPC construction. The effect of these improvements on radiation-induced noise was examined in the second test series.

The major changes in the board design used for the second test series were as follows:

(1) The UMPC transformer was recessed into the board such that the top rf shield was flat with respect to the top of the board (fig. 8). This more closely approximates the planned installation of the transformers in future test articles.

Figure 8. Installation of current transformers into circuit board for test-series 2 and 3. Heavy lines indicate copper; remainder is dielectric. Not shown are copper covers attached to planes on top and bottom.

Cutout top layer
0.200 × 0.350 in.

Cutout top layer 2, 3, 4
0.130 × 0.180 in.

Wire bonding level

0.200 × 0.350 in.

0.093 in.

Top plane
0.030 Layer 2 SIG
0.030 Layer 3 plane
0.030 Bottom plane

0.130 × 0.180 in.

17
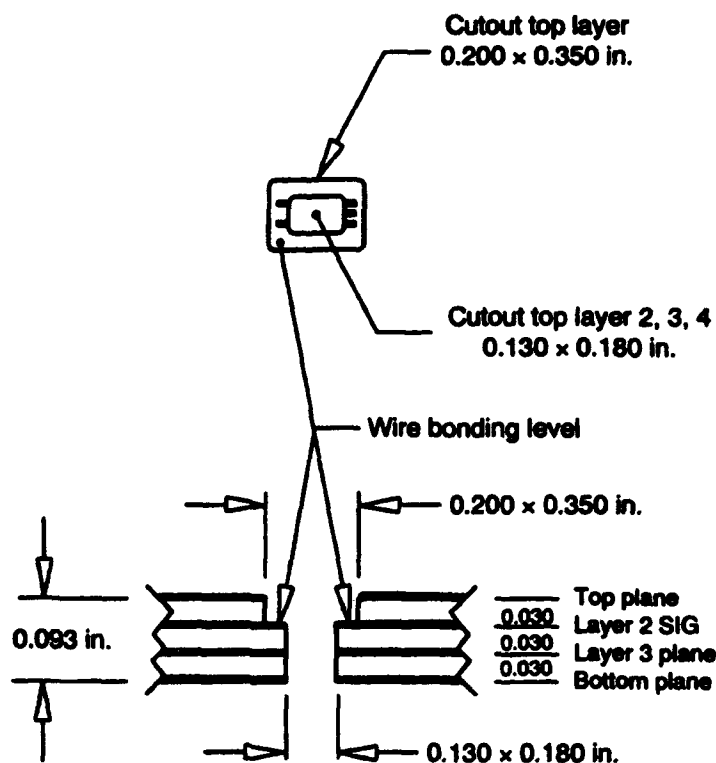
(2) The top and bottom of the rf enclosures were silver-epoxied to the respective ground planes (and not soldered as was previously done). This was to minimize any effect due to excessive heating of enclosures, which are silicone coated internally.

(3) Line lengths were carefully balanced for each pair of leads. Additionally, the balanced leads were located close together, equalizing the radiation environment seen by them.

(4) "Dummy" transformers, consisting of ceramic carriers (see fig. 3) without windings, were included to evaluate the noise induced into connections. The flywires and potting were the same as with operating transformers.

(5) Various patterns of unconnected test board traces (for instance figs. 7(a), 8(a), 8(b), and 9) were provided to allow an evaluation of the noise contribution of traces in the VTS board.

The transformer constructions tested in the second and third test series were as follows:

(1) Types 1 through 5, inclusive, are electrically the same as those of the first test series, using a single ferrite bead and a termination resistor, but with different types of encapsulants.

(2) Type 6 is a "dummy" used to check the package response, exclusive of the transformer windings.

(3) Types 8 through 10, inclusive, use two ferrite beads (increasing the inductance) with a common winding, but without the 50-Ω resistor across the output leads. The L/R ratio remains satisfactory because of the increased inductance. The absence of the resistor, with its charge-collecting surface area, was expected to decrease noise under radiation.

(4) The transformer in board location D (see fig. 9) is connected by 5-mil traces; all other traces are of the standard 10-mil width. Type 7 is a thermistor, used for temperature measurement, and is not a subject in these tests. These constructions are described in table 3.

A total of five test boards were made in which the various transformers, encapsulants, and board locations were permuted. The makeup of the boards is presented in table 4.

All boards, and therefore all combinations of construction shown in table 4, were exposed to HIFX and the results recorded by methods similar to those employed in the first test series. In the second test series, as in the first, no lead collimation is used; the full face of the test board was illuminated.

18

Figure 9. Current transformers on test board for tests of series 2 and 3. Unconnected traces, such as 5A and the unconnected Pogo connection 4A, are used to determine the induced noise picked up by the traces themselves, exclusive of effects on the transformer's conductors.
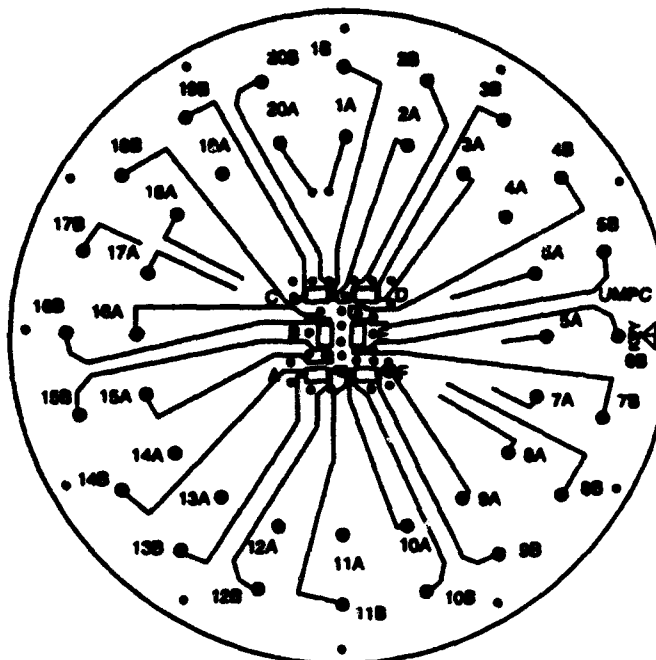
Table 3. Construction of UMPC transformers tested in test-series 2 and 3.

UMPC type	UMPC description		Quantity (5 boards)
	Components	Encapsulant	
1	Ferrite + resistor	2850 FT (blue)[1] only	4
2	Ferrite + resistor	Silicone spray[2] + 2850 FT (blue)	3
3	Ferrite + resistor	Ablebond 69-5 epoxy[3] only	4
4	Ferrite + resistor	Ablebond 933-1 epoxy[3]	4
5	Ferrite + resistor	Rigid Hipec (Q1-4939)[4]	3
6	None (dummy)	Flexible Hipec (6646)[4]	2
7	Thermistor only	Flexible Hipec (6646)	2
8	Two ferrites, no resistor	2850 FT (blue)	3
9	Two ferrites, no resistor	933-1 epoxy only	3
10	Two ferrites, no resistor	Flexible Hipec (6646)	2

Encapsulants:
[1]*Emerson & Cummings;* [2]*Miller Stephenson MS 460;* [3]*Ablestik;* [4]*Dow Corning*

Table 4. Matrix of UMPC transformer types on test boards of test-series 2 and 3.

Board location	UMPC type				
	Board No. 1	Board No. 2	Board No. 3	Board No. 4	Board No. 5
A	1	10	10	3	4
B	2 (Driven)	4 (Driven)	5 (Driven)	1 (Driven)	3 (Driven)
C	2	4	5	1	3
D (5 mil)	2	4	5	1	3
E	7	7	8	8 (Driven)	9 (Driven)
F	6	6	9	8	9

Note that no Pogos containing current transformers were used in the second and third test series; it was felt that no additional data would be yielded by them, and recording channels were scarce. In the first test series the transformer-equipped Pogos held no surprises: they only verified the test signal current into the current probes (already known from a monitoring oscilloscope used during setup) and indicated the total IEMP drive to the board traces and current transformer.

In the second and third test series the trace IEMP drive was monitored separately, via the unconnected traces. It was expected that the IEMP drive to the board traces connecting to the transformer would be the same in the second test series as it had been in the first series; the length of the traces was altered only slightly and the board construction was identical.

The IEMP drive to the traces is presented first because it affects the interpretation of the current transformer noise measurements. It will be seen that the IEMP drives are less consistent with trace surface areas than might be expected, and that in general the balance between IEMP drives to closely-spaced equal length (and width) lines is not as close as one would expect. This leaves open the possibility of significant noise injection via the "balanced" lines on the test board. The noise from the cujac cables and Pogos was determined to be inconsequential; they are not a part of the noise background.

The following analysis of the noise contribution of the traces, and of course the associated Pogos and their cujac lines, is broken into three parts: (1) Pogos and cujacs, (2) contact pads (the circular board area contacted by the Pogos), and (3) the traces attached to the contact pads.

5.2   Pogo and Cujac Noise

For these tests the Pogos were insulated from the test board by a Mylar sheet, and HIFX was operated at maximum charge, spaced closely to the test board, with no Pb shielding collimator; the dose rate was about 4×10^{11}. The cujacs connected to the Pogos were directly connected to the 50-Ω digitizers. The V-type Pogos (the only type used in the second and third test series) were found to have negligible noise levels. When a V-type Pogo was placed in the outer ring of Pogos, its noise level was less than 1 mV (into 50 Ω)—i.e., less than 0.02 mA. When the Pogo was in the inner ring, the noise level averaged about 2 mV, with the maximum being 5 mV (0.1 mA).

5.3 Contact Pad Noise

Table 5 presents the measurements of contact pad noise. When a Pogo contacted the small (2-mm-diam) pad on the test board, the noise increased from less than 0.1 mA to the range of 0.16 to 1.1 mA, depending on the DC bias voltage and whether the pad was in the A or B ring. This is a larger than expected response, considering the small area of the 2-mm-diam pad and that the radiation level at the pad, about 4×10^{10}, is about 1/10 that at the center. The radiation level, adjusted by changing the distance to HIFX, had a modest effect, far less than linear. These results for contact pads demonstrate that one must be careful about the location and coating of chip resistors and other components on the test boards; their area is somewhat larger than that of the Pogo pads and they would therefore be expected to receive an IEMP drive of at least a milliamp or so, even when located near the periphery of the board, the area receiving the least radiation.

5.4 Trace Noise

The final step in determining the noise contribution of the trace areas on the board connections was to measure the IEMP to representative examples, including, unavoidably, the connecting pad and Pogo. The test board of figure 9 contains eight unconnected traces, identified by their connection to Pogo pads 5A, 6A, 7A, 8A, 8B, 17A, 17B, and 18A. The IEMP currents received by these traces were measured for various conditions of DC bias and at both high ($\sim 2 \times 10^{11}$) and low ($\sim 5 \times 10^{10}$) radiation levels. Attention was concentrated on equal length pairs, of which 17A and 18A, and 6A and 7A were the best pairs in that they were close together. The importance of these pairs is that their response, including the degree of balance between them, exemplifies that of the balanced traces connecting to the secondary of current transformers.

The results for the pairs of traces are shown in table 6. In this table all readings are for traces with a 0-V DC bias; this is of primary interest

Table 5. Current collection by unconnected Pogo pads, whose locations are shown in figure 4.*

Pad	−55°C				25°C				125°C			
	$\sim 5 \times 10^{10}$		$\sim 2 \times 10^{11}$		$\sim 5 \times 10^{10}$		$\sim 2 \times 10^{11}$		$\sim 5 \times 10^{10}$		$\sim 2 \times 10^{11}$	
	0 V bias	+15 V	0 V	+15 V	0 V	+15 V	0 V	+15 V	0 V	+15 V	0 V	+15 V
7A	−24	—	−20	—	−34	—	−32	—	−25	—	−20	—
18A	−32	—	−30	−45	−22	−48	−50	−55	−55	−45	−30	−50
18B	−8	—	−12	−20	−10	—	−13	−22	−12	−18	−8	−20

*Bias on pads either 0 or +15 V as indicated. Radiation level indicated is at center of board (location of transformers under test). Units are mV across 50 Ω—i.e., mA × 50.

Table 6. Radiation-induced noise response of traces in circuit boards for two radiation levels and three temperatures. Location of traces shown in figure 9. Radiation level indicated is at center of board. Units are mV across 50 Ω—i.e., mA × 50. Trace bias is 0 V.

Trace (see fig.10)	Board No.	$-55°C$ $\sim5 \times 10^{10}$	$\sim2 \times 10^{11}$	$25°C$ $\sim5 \times 10^{10}$	$\sim2 \times 10^{11}$	$125°C$ $\sim5 \times 10^{10}$	$\sim2 \times 10^{11}$
17A (10 mils)	1	-64	-50	-50	-44	-60	-48
	2	-38	-56	-48	-60	-58	-64
	4	-65	-43	-63	-65	—	-58
18A (5 mils)	1	-60	-50	-64	-56	-63	-55
	2	-60	-48	-67	-57	-64	-50
	4	-55	-46	-68	-60	—	-57
6A (10 mils)	1	-28	-18	-25	-20	-26	-22
	2	-24	-20	-30	-22	-23	-22
	4	—	—	—	—	—	—
7A (10 mils)	1	-31	-25	-36	-27	-32	-25
	2	-30	-26	-40	-31	-35	-27
	4	-30	-23	-40	-32	—	-26

because that is their bias condition when they are used to connect to the output of a current transformer.

An unexpected result was that trace 17A, which is 10 mils wide, received nearly the same current drive as 18A, which is 5 mils wide. About half this current was presumably from the Pogo pad (see sect. 5.3), but it is apparent that the wide and narrow traces received about equal drives.

It can also be seen that the shorter traces (figs. 6(a) and 7(a)) received little more drive than did the Pogo pads; apparently the IEMP drive to traces near the periphery of the board was small. The area of the traces was about 3.7×10^{-3} in.^{2}; the total surface area was increased about 50 percent above that of a Pogo pad alone.

Note that the current drive did not in any way follow the radiation level; when the test fixture was moved away from HIFX in order to decrease the dose rate from $\sim2 \times 10^{11}$ to $\sim5 \times 10^{10}$, the drive in many cases increased. A similar lack of tracking of IEMP current (or whatever the traces and pads are collecting) with radiation level is shown in table 5.

The boards to which the current transformers were attached did not contain unconnected traces extending nearer to the center of the board than do 17A and 18A. The marked increase in collected current between 6A,7A and 17A,18A suggests that the additional increment of length between, say, 17A and a conductor extending to the center of the board, the location of a transformer, would intercept

considerable current. Information about the current collected by such long traces was gained from two sources: (1) "dummy" probe locations, which include traces extending to the board center (but also the flywires of the ceramic transformer support) and (2) current to an unconnected buried trace extending to near the center of a test board used during a previous test. The data regarding the former (1) will be presented in detail in section 5.5. The results for the buried trace are presented in table 7. The peak current on this trace was considerable, as much as 3 mA, even at 0-V DC bias (as are the current transformer connections). This result is in reasonable agreement with the current-drive value measured in a series-1 test board, shown previously in section 4.1.

5.5 Dummy Transformer Noise

In all the second test series, the entire front of the board was exposed to HIFX. This means that the board traces connecting to the transformers were fully irradiated. In order to determine the noise contribution of these connections, two of the test boards contained dummies of transformers. These consisted of the ceramic mounting of figure 4, but with no components attached to it, connected to the board exactly as are the transformers.

Note that in all measurements following in this report no conductors were placed through the current transformers; no current is applied—the output signal is entirely noise. An external signal, from a square-wave generator, was only applied in the (preceding) first series of tests.

Table 8 presents the measured noise values for these dummy packages ("transformer" F of boards 1 and 2), as well as for the actual

Table 7. Radiation-induced noise response of long circuit board trace (indicated by arrows in figure at right), extending to center high-radiation area of circuit board. Radiation level indicated is at center of board. Units are mV across 50 Ω—i.e., mA × 50. Board is fully illuminated (no collimator).

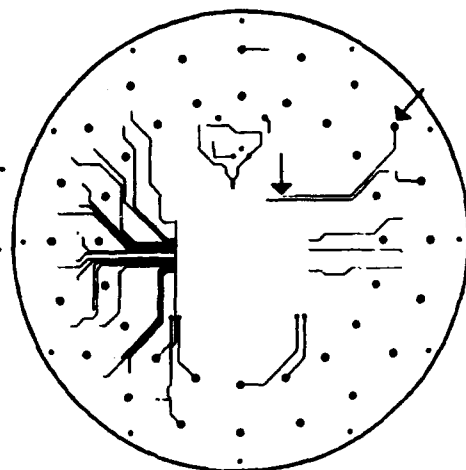| Dose rate (rads(Si)/s)	Temperature (°C)	Bias (V)	mV across 50 Ω (mA × 50)
4×10^{11}	25	0	−150
4×10^{11}	25	+5	−150
1×10^{11}	25	+5	−100
5×10^{10}	25	0	−50
5×10^{10}	25	+5	−50
4×10^{11}	−55	+5	−250
4×10^{11}	+125	+5	−300

Table 8. Radiation-induced noise output of UMPC transformers in test-series 2. *

Board No.	Temp (°C)	UMPC transformer					
		A	B	C	D	E	F
1	25	-5	+30	+6	+5	pkg = -7 mA	
1	-55	-6	>+30	+12	+4	pkg = 8 mA	
1	+125	-6	-4	-2	+8	pkg = -14 mA	
2	25	—	-2	-6	+4	pkg = 6 mA	
2	-55	—	—	-8	-2	pkg = -10 mA	
2	+125	—	+6	-10	-2	pkg = 2 mA	
3	25	-4	-10	+6	+10	+3	-3
3	-55	-4	-16	±3	+8	-4†	-4
3	+125	-6	-12	+6	+8	+3	-3
4	25	-6	+4	-2	-7	-1	+4
4	-55	-6	-2	-8†	-8†	±3	-5†
4	+125	-8	-4	-5	+8	+4	-3
5	25	+3	-8	-10	+6	-4	-4
5	-55	-6†	+4	-12	+6	-4	-4†
5	+125	-6	-3	-7	+6	-2	±3

*Radiation level indicated is at center of board, no collimator. Units are mA, taking into account balun loss. Values marked "pkg" are for a ceramic carrier with no transformer attached; the measured noise signal is that picked up by the carrier, flywires, and board traces.

†Indicates that the noise signal was time-stretched to a duration significantly greater than radiation duration.

transformers. The dose rate was approximately 2×10^{11} in all cases. It is seen that the measured dummy transformer noise signal was considerable, as much as 14 mA, with an average (absolute) value of about 8 mA. These measurements should be considered in the context that the calibration factor of the typical (one core) UMPC is 2.4 mA/mV, including the effect of the balun; the measured noise therefore represents the signal that would be produced by a current of (peak) 17 mA or (average) 10 mA flowing through the primary of a single-core UMPC. For the type 8, 9, or 10 UMPC (two cores), with a calibration factor of 0.8 mA/mV, the equivalent noise level averages 2.5 mA with a peak of 5 mA.

5.6 UMPC Transformer Noise

Table 8 also shows the responses of "real" UMPC transformers. To interpret table 8, recall that tables 3 and 4 relate the transformer location and board number to type of construction; for instance, transformer A on board 1 is a UMPC of type 1 construction: single ferrite core, 50-Ω internal load resistor, potted into the VTS board with blue encapsulant. It is readily apparent from table 8 that the induced

noise does not reach the hoped-for 1-mA level. It is also seen that low-temperature performance continues to be a problem; a number of the transformers have their greatest noise at this low temperature, and the noise-pulse stretching seen in the first series is again present in six of these transformers.

Figures 10 to 12 show the responses of three transformers as the temperature was varied. The traces are placed in order of consecutive shots, including two temperature steps (25° to –55°C and –55° to +125°C) in an attempt to delineate the onset and decay of stretching as the temperature was changed. The "H" or "L" at the lower corner of each trace indicates ~2 × 10^{11} or ~5 × 10^{11} rads(Si)/s.

Transformer C (fig 10) shows an erratic occurrence of stretching in consecutive low-temperature shots, and transformer F (fig. 11) consistently stretches at low temperature. Transformer A (fig. 12) seems unaffected by temperature changes. The reason for this (atypical) lack of temperature response could not be found.

The shape of the stretched response does not seem consistent with any electronic effect, such as cable reflection. In any case, the electrical integrity of the probe, Pogos, and cujacs was checked by a round-trip signal injection, as described previously in section 3.4, and no faults were found.

Figure 10. Radiation-induced noise response of a type 1 (single-core) transformer on consecutive shots as temperature and radiation level are varied; "H" denotes about 2 × 10^{11} and "L" about 5 × 10^{10}. Shots far too numerous to be shown here demonstrate that the time-stretched responses clearly visible in C, E, and G are frequent at low temperature and do not occur at other temperatures. Transformer is "C" on board 4.

25°C   H   25°C   H   –55°C   L

–55°C   H   –55°C   L   –55°C   L

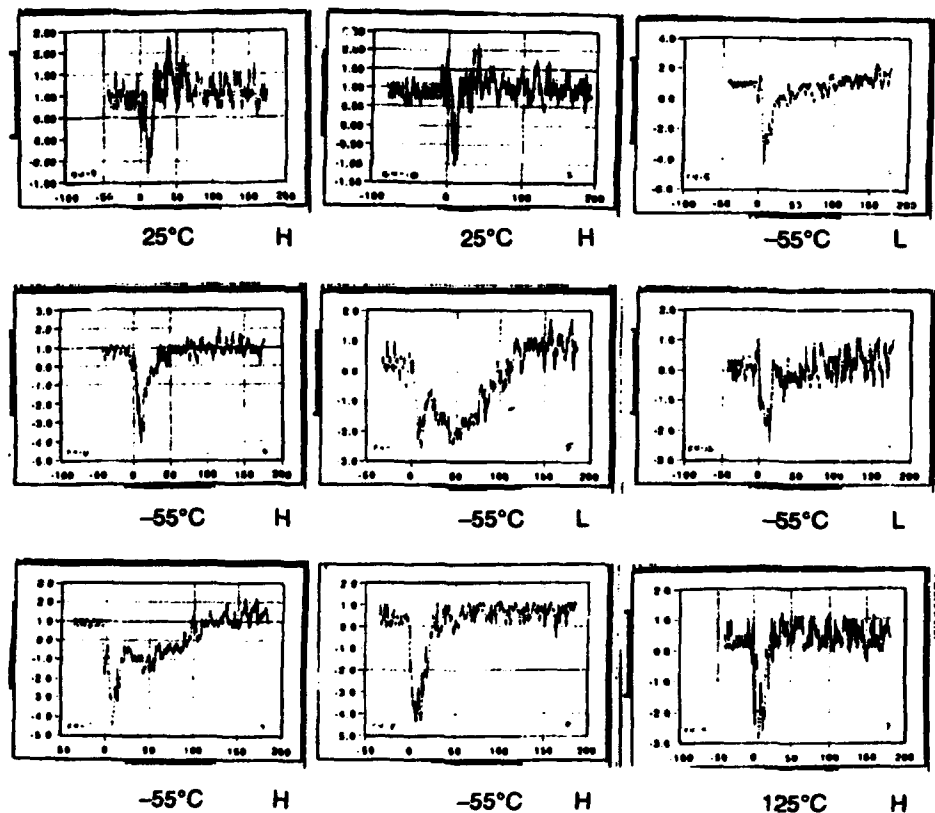–55°C   H   –55°C   H   125°C   H

Figure 11. Radiation-induced noise response of type 8 (two-core) transformer on consecutive shots as temperature and radiation level are varied. "H" denotes about 2×10^{11} and "L" about 5×10^{10}. As in figure 10 a stretched and increased response is produced at low temperature. Transformer is "F" on board 4.

25°C H	−55°C H	−55°C H
−55°C L	−55°C L	−55°C H
−55°C H	125°C H	125°C H

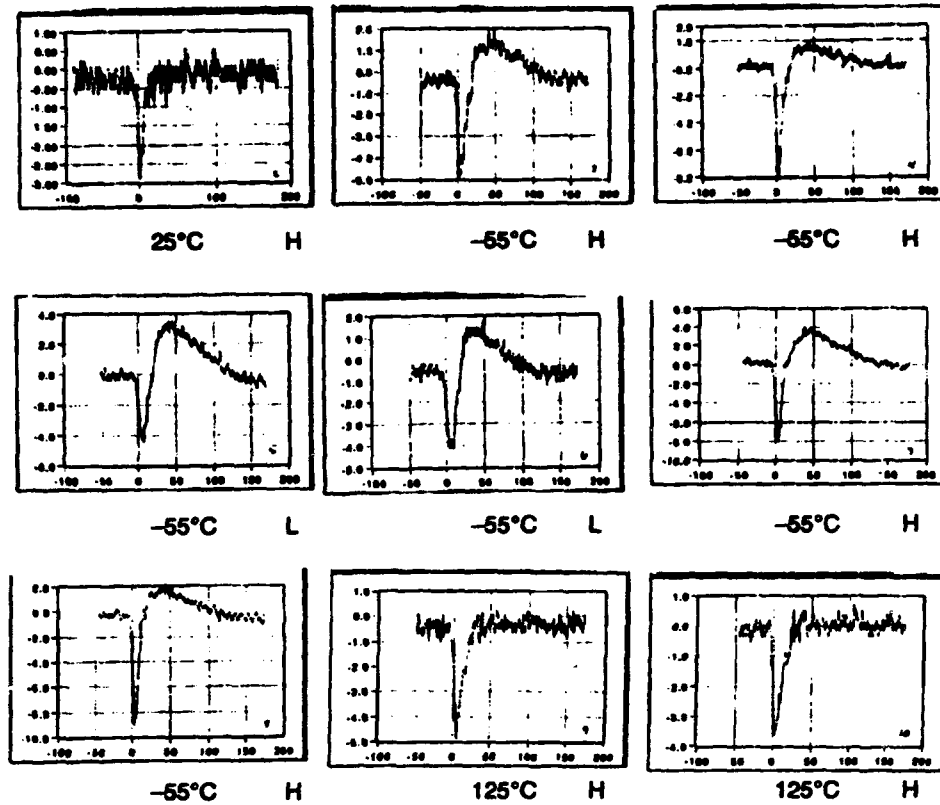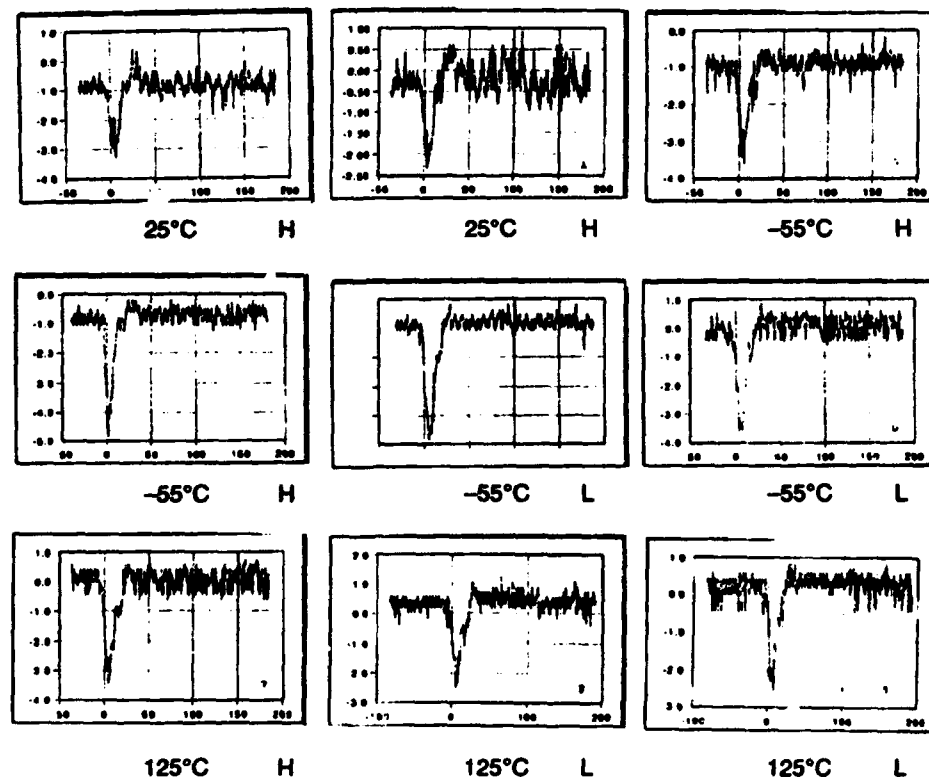Figure 12. Radiation-induced noise response of type 1 (single-core) transformer on consecutive shots as temperature and radiation level are varied. "H" denotes about 2×10^{11} and "L" 5×10^{10}. No effect is seen as temperature is varied.

25°C H	25°C H	−55°C H
−55°C H	−55°C L	−55°C L
125°C H	125°C L	125°C L

26

Returning to table 8, it seems that the worst noise performance, excluding transformer B of board 1, which seems anomolous, is shown by 3B, 1C, 2C, and 5C; these are all of different construction, save for the common factor of being single core, with an internal 50-Ω resistor.

Transformers 4E, 2D, 3F, and 5E are the best performers. Among these the construction of types 8, 9, and 10 (two cores, no internal resistor) is represented three times.

The conclusion is that the dual-core transformers have a lower equivalent noise level than the single-core, and that the effect of other construction details is ambiguous.

5.7 Balanced-Line Transfer Impedance and Noise

It was clear from the results of section 5.4 that one could not assume equal, and therefore compensating, drives to the transformer connections; they were therefore a significant source of noise.

The effective impedance at the current transformer's output terminals was not known, so an arrangement as depicted in figure 13 was used to relate unequal currents induced onto the balanced lines to the indicated current response. The pulse generator was terminated by the 51-Ω resistor, and low inductance 1000-Ω resistors (chip type) were used to drive current into one or both of the transformer output terminals (B),(C) at the VTS test-board Pogo connections. These Pogo connections were also connected by short cujac cables to a balun, and the balun output was recorded as a function of the current drive.

Figure 13. Method of measuring response of UMPC-balun system to an un- balanced current drive on interconnecting transmission line.

27
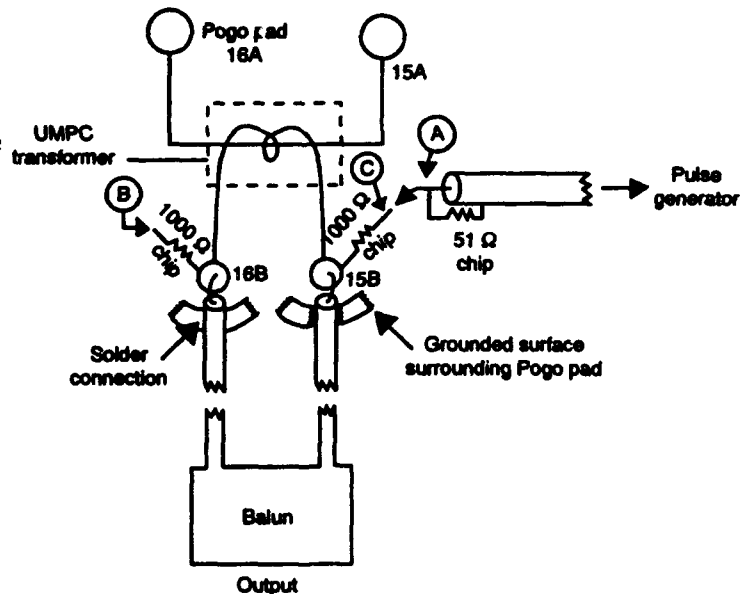
We found that for single-core transformers 1 mA of unbalanced noise drive (produced by pulsing Ⓒ to 1 V) created a 10-mV output from the balun; this is equal to what would be produced by a current of about 24 mA in the primary. If both connections were driven equally (by connecting Ⓐ to both 1000-Ω resistors Ⓑ and Ⓒ) the output returned to zero, as it should. Shorting the inputs (15A to 16A) had no appreciable effect—the response was not dependent on the input circuit to which the probe was attached.

The double-core transformers had a noise response about 1.6 times as great as that of the single-core devices; a 1-mA unbalanced drive produced about 16 mV of noise from the balun.

5.8   Discussion of Results

Referring to table 6 we see that noise-drive inequalities amounting to 0.1 to 0.2 mA (5 to 10 mV into 50 Ω) are frequent between pairs of traces on the VTS board. Relative to the single-core transformers these would manifest themselves as an apparent input current 24 times as great—2.4 to 4.8 mA; this is near the range typically seen for noise in the single-core transformer systems of table 8.

The increased noise-drive response of the two-core transformer is offset by its current response, which is over three times as great, at 1.5 mV/mA (versus 0.45 mV/mA). The net result is that the noise response in terms of primary current is about half as much as for the single-core UMPCs. The noise response shown in table 8 is also roughly one-half.

The sensitivity of the UMPC system to unbalanced current drive to the conductors within the test board suggested that the measured UMPC noise responses were not driven by the transformer itself, but rather by the board. In the next phase of tests (series 3) apertures were used to attempt to allow radiation to fall only on the transformer and its immediate surroundings, excluding the effects of the conducting traces in the test board.

6. Third Test Series

6.1   General Discussion

The final (test-series 3) step in evaluating the UMPCs was to irradiate selected ones through radiation-collimating apertures in an attempt to avoid the noise contribution of the interconnecting traces. The noise response of traces alone was also measured with the collimated beam. A complete beam-stopping shield was also used in a few instances to establish the noise floor (which was found to be

suitably low). Only a small number of tests were possible, since only a single day of shooting could be worked into the HIFX schedule. These tests were conducted at 25°C both to avoid possible heating/ cooling damage between shots and to speed up the shot rate. Figure 14 shows the arrangement of the collimator between HIFX and the transformers on the test board. The collimator consists of a 1-in.-thick Pb slab with either a 3/4- or ?-in. opening. The inner surfaces of the opening and the surface facing the transformer are covered with 0.05-in.-thick aluminum to stop the electrons emitted from the high-Z Pb. In use, the 3/4-in. opening is centered in front of an individual transformer and the 3-in. opening is centered with the board; it is large enough to include all transformers.

The maximum obtainable fluence was reduced because of the increased separation between t..ansformer and HIFX which was necessary to insert the collimator. TLDs monitored the actual dose rate obtained under these test conditions and showed the typical incident fluence to be about 1×10^{11} when the 3-in. aperture was used and 8×10^{10} with the 3/4-in. aperture.

6.2 Transformer Noise

In test-series 2 (no collimation) transformer 3E was among the lowest in noise of the two-core types, and therefore among the lowest in

Figure 14. Placement of "collimator" between HIFX and board carrying UMPC transformers. Dose-measuring TLD's are located on board, centered with collimator opening. For reduced radiation level the collimator remains in same location relative to HIFX and the board is moved away from both.
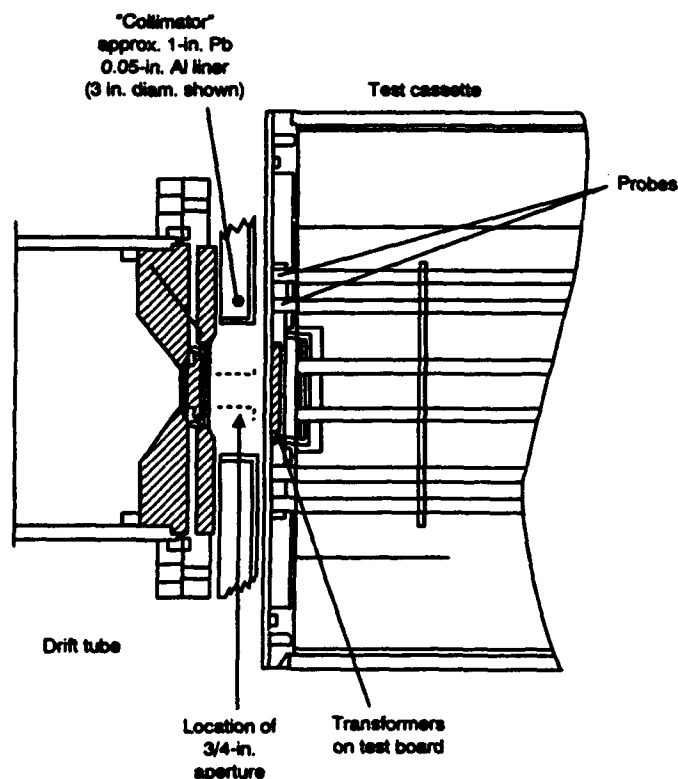
noise of all the transformers. As shown in table 8, its noise level was equivalent to about 3 mA when exposed at 3×10^{11} with the connecting traces unshielded by Pb. When exposed through the 3-in. aperture the noise level peaked at less than 1 mA; this is reduced by about the same ratio as the fluences. When exposed through the 3/4-in. aperture the noise level dropped only a little, relative to the results with the 3-in. aperture. These results imply that (1) the lines are in this case not a major contribution to the noise (the noise is hardly affected by irradiating about 1/2 the length of the line traces on the board as opposed to their full length) and (2) therefore the noise seen is a product of the transformer and its immediate connections. The noise level of transformer 3E itself is about 0.7 mA at 8×10^{10}, determined by the measurement through the 3/4-in. aperture. It would therefore be about 2.5 mA at the 3×10^{11} level obtained in test-series 2. Recall that these results are for 25°C.

Another two-core transformer, 4F, was not quite as low-noise as 3E in test-series 2, but it was exposed to a more complete range of radiation conditions in test-series 3. Figure 15 shows results for irradiation through 3/4- and 3-in. apertures, no aperture (full board exposed), and with a full Pb shield (virtually no radiation). The progressively larger noise level as the aperture increases implicates the interconnecting traces as a significant noise source. Trace 15A, with negligible radiation, illustrates the electronic noise level; although digitization noise is apparent, the deviation at radiation time appears to be less than 0.5 mV.

Figure 15. Radiation-induced noise response of two-core transformer 4F with several conditions of collimator aperture/shielding. The peak radiation level is about 1×10^{11} for 15B–15D.

A. No radiation, fully Pb shielded

B. Irradiated through 3/4-in. aperture

C. Irradiated through 3-in. aperture
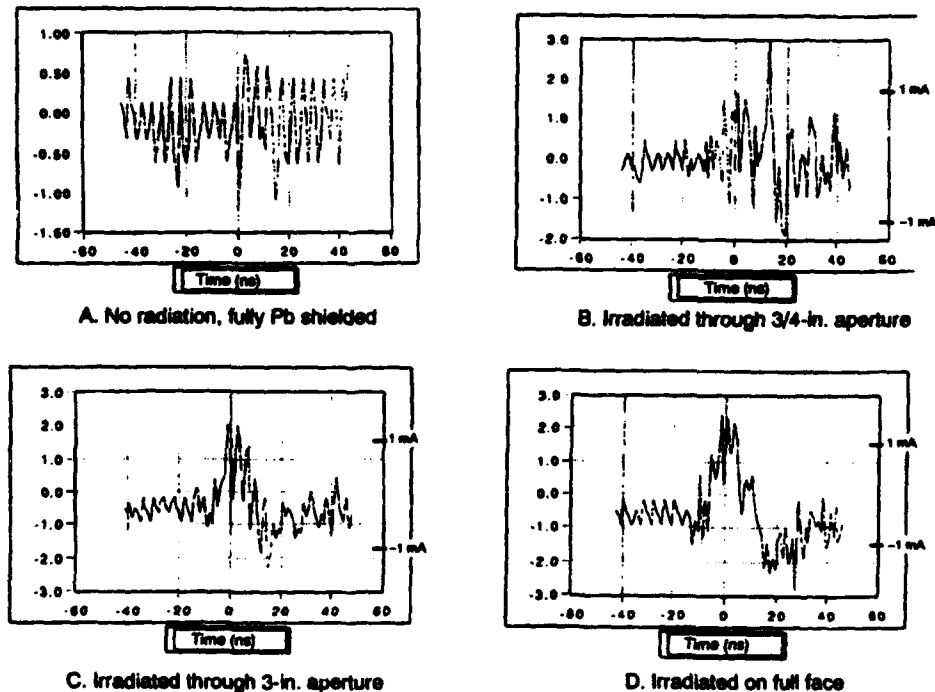
D. Irradiated on full face

30

Figure 16 shows results for single-core transformer 2C, one of the lowest noise single-core units in the second test series. The results are similar to those seen for 3E. The noise level is little affected by increasing the aperture size and irradiating larger lengths of the balanced line on the board. The noise level is therefore presumed to be primarily that of the transformer itself. The noise response is about 2 mA at 1×10^{11}.

Figure 17 is the performance of a high-noise single-core transformer, 1C, through apertures. An increase in noise is visible as the aperture is increased, showing that the noise picked up by the board traces is a contributor.

The preceding paragraphs, describing the series-3 test results, lead to the same conclusion reached in the series-2 tests: The noise contribution of the balanced (at least geometrically) lines connecting to the trans'·rmer is likely the determining factor in the UMPC system

Figure 16. Radiation-induced noise response of single-core transformer 2C with several conditions of collimator aperture/shielding. The peak radiation level is about 1×10^{11} for 16B–16D.

A. No radiation, fully Pb shielded

B. Irradiated through 3/4-in. aperture

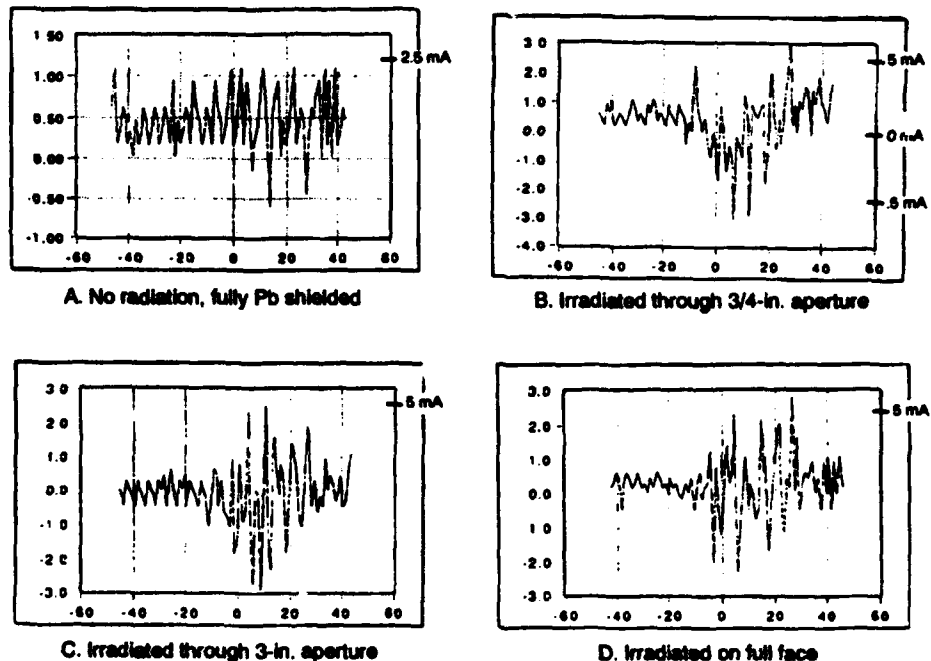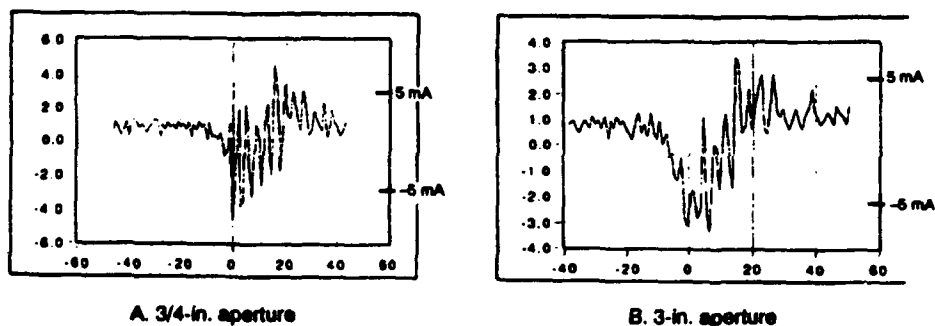C. Irradiated through 3-in. aperture

D. Irradiated on full face

Figure 17. Radiation-induced noise response of single-core transformer 1C irradiated through 3/4- and 3-in. apertures. Dose rate about 1×10^{11}.

A. 3/4-in. aperture

B. 3-in. aperture

31

noise. In those cases where system noise was found to be low and not strongly dependent on the area irradiated—for instance, transformer systems 3E and 4C—it is likely because the lines happen to receive equal drive, and these drives cancel in the balun. Under these conditions the observed noise is assumed to approach that of the transformer itself. This noise can be quite low, less than 1 mA at 8×10^{10}, and is estimated as about 2.5 mA at 3×10^{11}.

6.3 Trace Noise

Pogo pad and trace noise were also observed during test-series 3. It is useful to look at the drive received by traces 17A and 18A (the balanced pair connected to Pogo pads in the A ring), 8B, a single trace connected to a B-ring Pogo, and 4A, a Pogo pad alone. These are the same traces and Pogo pad monitored in the series-2 tests. Figure 10 shows their location.

Figure 18 presents the IEMP drives to the pair 17A,18A (expressed in mV into 50 Ω). Recall that 18A is 5 mils wide and 17A 10 mils wide, as are all other board traces. Figure 18(a) shows the drives with the 3/4-in. aperture aligned with transformer 4F, at the opposite side of the board from 17A and 18A (see fig. 9), and the drives are similar in magnitude, but of different polarity. The thinner trace, 18A, receives somewhat more drive. When the 3/4-in. aperture is aligned with transformer 4C, near the ends of 17A and 18A, the drives are increased. It is still of opposite polarity, and the 5- and 10-mil traces still receive nearly equal drive magnitudes (fig. 18b). When the 3-in. aperture is used, illuminating the center half diameter of the board, the drives become larger and highly unequal in magnitude, although of the same polarity (fig. 18c). Again, the narrower trace receives more drive. Finally, the collimator is removed and the entire board face is illuminated. The drives increase somewhat more, with the drive to 18A saturating the digitizer. We see once again that neighboring traces do not necessarily receive drives proportional to their area, or even drives of the same polarity.

The response of trace 8B, which is most nearly the same as the traces connecting the UMPC secondaries to the Pogo, is shown in figure 19. It shows increasing drive as the aperture is moved nearer to it or expanded in size.

The response of Pogo pad 4A is not shown as a figure. Suffice it to say that it receives little drive with any of the collimators in place—not surprising since it is about 1 in. from the opening of even the large 3-in. collimator. When the collimator is removed the drive is similar to that observed in test phase 2 (see table 5).
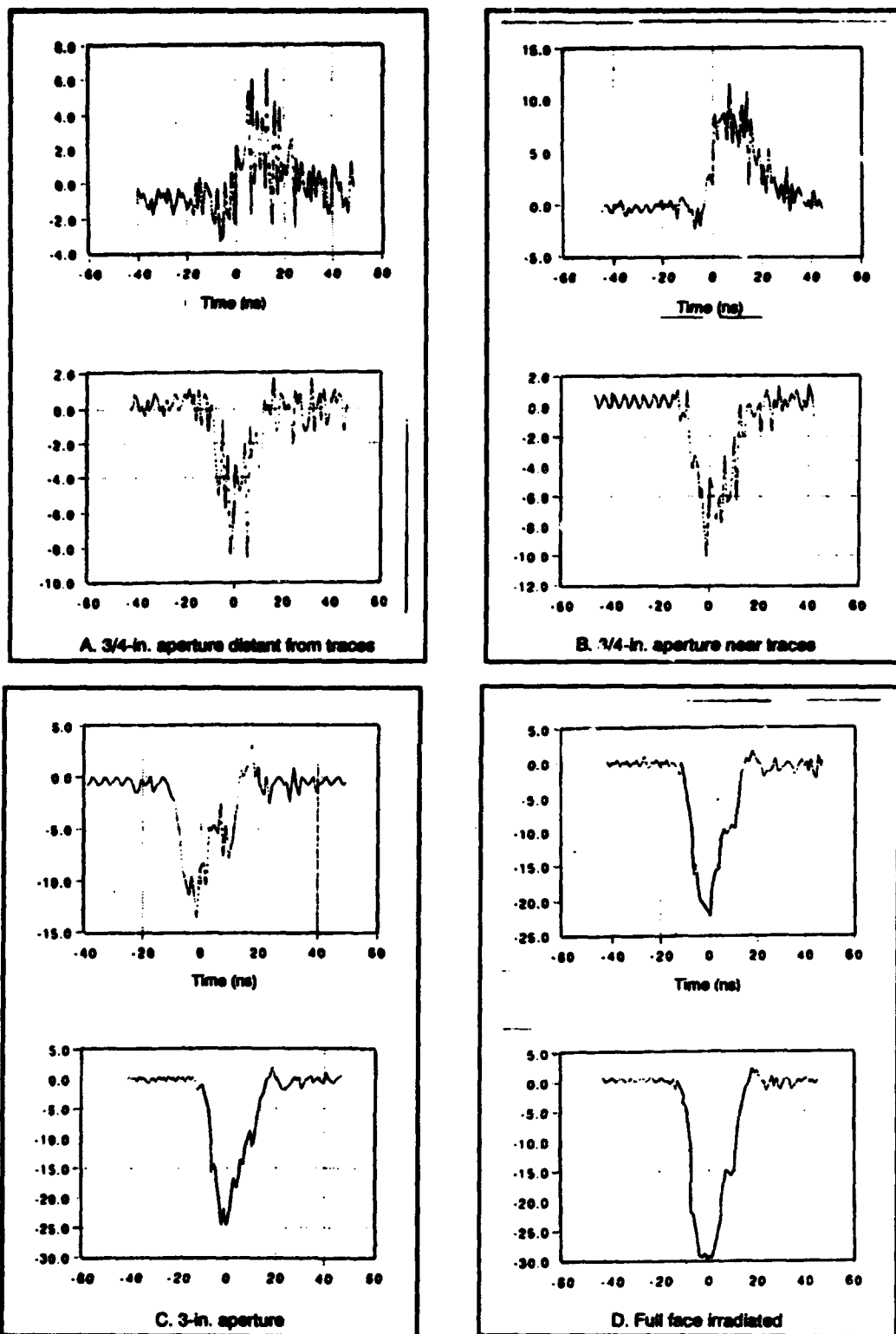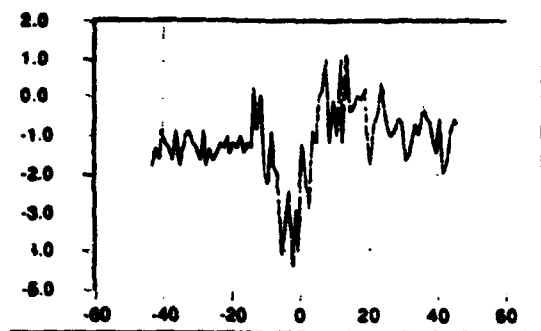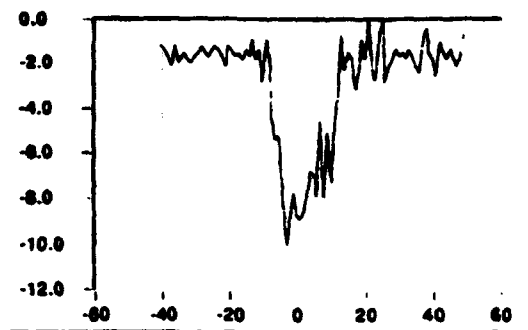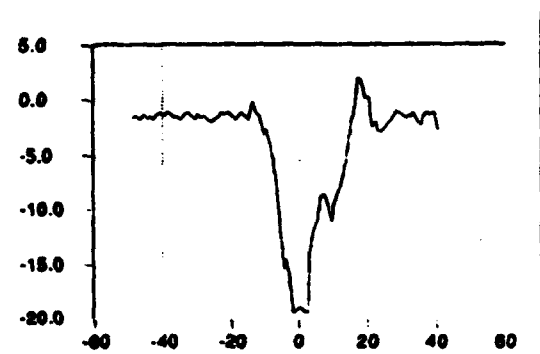
Figure 18. Radiation-induced noise voltages on traces 17A and 18A (a "matched-pair;" see fig. 9) as collimating aperture size and location is varied. In the four pairs of traces 17A is upper and 18A lower. Note that the voltages do not remain equal, in spite of the identical sizes and close colocations of the traces.
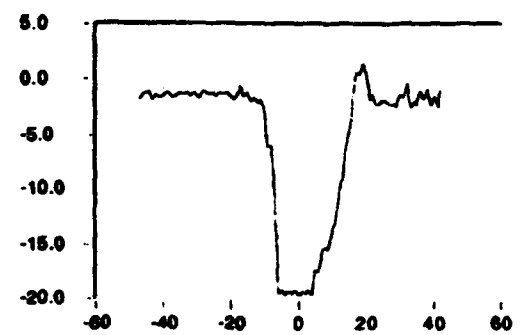
33

A. 3/4-in. aperture distant, aligned with transformer C

B. 3/4-in. aperture near end of trace, aligned with transformer F

C. 3-in. aperture

D. Full face irradiated

Figure 19. Radiation-induced noise voltages on trace 8B (see fig. 9) as aperture size and location are varied. This trace is much like those connecting the transformer outputs to instruments; it is 10 mils wide and connects to a B-ring Pogo, whose noise level into 50 Ω is typically less than 1 mV.

7. Conclusions and Comments

The original purpose of the study was to determine what types of UMPC transformer constructions (potting compounds, number of cores, etc.) were best with respect to noise. The conclusion has already been stated: the two-core type provides a lower noise. This seems to be little affected by construction details such as potting materia... The lack of the internal load resistor is presumably the reason: without it the transfer function is increased, with a greater signal output produced for a given input current; any noise contribution from IEMP onto the connecting traces is proportionately decreased.

There was a decided improvement in the performance of even the single-core transformer of the second set (test-series 2 and 3) relative to those first test series. This is likely because these were all developmental devices, and much more careful potting procedures and lower solder temperatures were used in constructing the second set.

It was not possible to determine with certainty the noise level of the transformer itself, since its output signal could never be entirely

34

divorced from the effects of the connecting traces on the circuit board. In some cases, such as those represented in figure 16, it appeared that the connecting traces contributed a minimal amount; the total noise level was sub-milliamp at about 1×10^{11} rads(Si)/s. The low trace-noise assumption also allows the data of table 8 to be taken as meaningful for the same transformers, in the higher dose-rate tests of series 2. The noise level of two-core units, 3E and 4F, is about 3 mA, with an incident dose rate of about 4×10^{11}.

An important finding is that the circuit boards do not provide a low or balanced noise drive to traces, even when the boards are fabricated carefully, with multi-layer geometrically balanced construction. The drive was not found to be necessarily proportional to either trace surface area or radiation level. Since this is so greatly at odds with expected results, where drive is proportional to area and dose rate, it would seem that some additional type of coupling, as well as direct IEMP drive, may be taking place between the radiation (or its source, HIFX) and the traces within the board.

It is useful to have determined (in sect. 5.7) the relationship between unbalanced noise drive to the transmission line connecting to the transformer and the equivalent primary current (that being measured by the transformer). Unfortunately the result shows that the transformer system is sensitive, that excellent balance is required to achieve a low noise level, and such equality of drive was not typically observed in the measurements of trace response.

The time-widened noise pulses seen at low temperature in figure 11 and elsewhere remain a mystery. They resemble the delayed current due to slow-moving secondary electrons being collected by charged surfaces, reported by Seider et al. [8], but in these UMPC experiments the bias on the lands connecting to the transformer outputs is always zero (within ±50 mV), and this would not produce the fringing-field which was necessary to cause their collection in those experiments [8].

8. Recommendations

It appears that more understanding of radiation-induced current drive to buried conductors is required, at least how to achieve equality in them. As stated earlier, many of the drives observed in these tests were not expected or explained with sufficient accuracy by the typical board IEMP criteria. It is recognized, however, that the goal of measurement of small currents imposes demands which are more stringent than required for typical circuits; for instance, almost no digital circuit would be significantly affected by the presence or

35

absence of a 2-mA circuit-board IEMP drive, yet this level is critical to the goal of input photocurrent measurements.

The sometimes totally unexpected noise levels, which in a device under test (DUT) would almost certainly have been mistaken for signals, demonstrate the necessity of including noise references in radiation test systems. We have seen that even when everything is scrupulously done "correctly," surprises occur. "Dummy" noise reference probes can alert the experimenter to a problem. A previous test demonstrating the value of such noise probes was a part of the Disco Elm UGT [9]. Here the noise-reference current probes showed that background noise was large, and therefore that data reported by the signal current probes were suspect. This led to the study of Blackburn et al. [2], which revealed that under some conditions the current transformers in use at that time had unexpectedly large noise responses.

Finally, I suggest that current probe instrumentation be supplied with a means to conveniently determine that the probe-line-balun system is intact. If one of the two balanced lines becomes detached, the signal will drop by 50 percent, but otherwise be little changed; this can easily be undetected (especially if the experimenter is without accurate prediction); meanwhile, the signal-to-noise ratio may have deteriorated to near zero, resulting in only noise being measured under radiation.

If unmatched tees are placed at balun inputs, a point for attaching a test signal is available: the open inputs to the tees. (Although only one tee is needed for this, the second retains the symmetry of the signal path.) If a pulse is applied to one of the tees (by a temporary connection), a characteristic signal will be seen at the balun output. This signal will depend on transmission-line length and type of transformer, but will be discernible from that obtained if the lines or transformer contain a broken path. Note that since no disconnection of connectors in the signal path is required for this test it avoids the possibility of a faulty reconnection, as can occur when a line is temporarily disconnected for tests and then reconnected. The short unterminated stub formed by the normally unused connection to the tee is inconsequential at the frequencies where the probes are used, appearing as a shunt capacitance of about 1 pF.

References

1. Dale Robertson, Marc Litz, Steven Blomquist, and James Blackburn, *Electron-Beam-Pinch Experiment at Harry Diamond Laboratories: Providing for a High-Dose-Rate Flash-X-ray Facility for Testing of Electronic Pieceparts*, HDL-TM-91-11 (August 1991).

2. James Blackburn, Jonathan Vanderwall, Dale Robertson, and Steven Blomquist, *Radiation-Induced Noise Response of the Jaycor MPC-8 Radiation-Hardened Current Probe*, HDL-TM-91-10 (August 1991).

3. W. Seidler et al., *Temperature-Dependent Dose-Rate Effects in CMOS/SOS Devices*, Paper B-7, HEART Conference (February 1992); to be published in Journal of Radiation Effects Research and Engineering (JRERE).

4. W. Seidler et al., *Scaling Box IEMP to High Fluences*, JRERE, 17, 1R (January 1989).

5. Private communication from G. Ovrebo (ARL) (October 1991).

6. Private communication from A. Smith (Ktech) (June 1991).

7. Private communication from W. Seidler (Jaycor) (September 1991).

8. W. Seidler et al., *Box IEMP Hardening Investigations, Vol. II, Inner Board Coupling and Secondary Electron Collection in Box IEMP*, Defense Nuclear Agency, DNA-TR-84-133-V2 (March 1984).

9. James Blackburn, Dale Robertson, Gregory Ovrebo, Steven Blomquist, *Disko Elm Active Electronics Experiment*, HDL-TR-2175-S (May 1992).

Distribution

Admnstr
Defns Techl Info Ctr
Attn DTIC-DDA (2 copies)
Cameron Sta Bldg 5
Alexandria VA 22304-6145

Director
Defns Nuc Agcy
Attn RAEE L. Cohn
Attn RAEE L. Palkuti
6801 Telegraph Rd
Alexandria VA 22310-3398

HQ US Army Special Oprn Comnd
Attn A. Gies
Attn DCS-FCI-CD-TB S. Raineri
Attn E. Blough
Bldg D3206 Rm 503
FT Bragg NC 28307-5200

Commander
Nuc Effects Lab
Attn STEWS-NE J. Meason
White Sands Missile Range NM 88002-5180

U.S. Army Corps of Engr
Attn CEHND-SY R. Johnson
Attn CEHND-SY J. Loyd
PO Box 1600
Huntsville AL 35807-4301

Commander
U.S. Army Sp & Strtgc Defns Comnd
Attn CSSD-SL-S I. Merritt
PO Box 1500
Huntsville Al 35807-3801

Director
US Army Sp & Strtgc Defns Comd
Attn CSSD-SD-A A. Kuehl
Attn CSSD-SD-AM C. Harper
Attn CSSD-SA-EV R. Bradshaw
Attn CSSD-SD-AM A. Corder
Attn CSSD-SD-AM G. Little
Attn CSSD-SD-AM K. Blankenship
Attn CSSD-SD-AM P. Adams
Attn CSSD-SD-AM R. Goodman
PO Box 1500
Huntsville AL 35807-3801

Commanding Officer
Nav Rsrch Lab
Attn C. Dozier
Attn Code 6816 W. Jenkins
Attn Code 8120 A. Fox
4555 Overlook Ave SW
Washington DC 20375-5000

Commanding Officer
Nav Weapons Spprt Cte
Attn Code 6054 T. Turflinger
Bldg. 2506
Crane IN 47522

Commander
USAF Sp & Mis Sys Ctr
Attn K. Basany/MBSPH
2400 E. El Segundo Blvd
PO Box 92960-WPC
Los Angeles CA 90009-2960

Arspc Corp
Attn M4/949 L. Mendoza
PO Box 92957
Los Angeles CA 90009-2957

Berkeley Rsrch Assoc Inc.
Attn D. Weidenheimer
Attn J. Deaver
PO Box 852
Springfield VA 22150

Harris Corp
Attn A. Sanchez MS19/4824
Attn R. Moss MS19/4824
Attn G. Chunn MS 19/4841
PO Box 9400
Melbourne FL 32901

Jaycor
Attn L. Ziegler
4950 Corporate Drive
Huntsville AL 35805-6221

Jaycor
Attn C. McKnett
2951 28th St Ste 3075
Santa Monica CA 90405-2976

39

Distribution

Jaycor
Attn S. C. Rogers
Attn B. Passenheim
Attn C. Mallon
Attn D. Bruener
Attn D. Walters
Attn E. Wenaas
Attn H. Harper
Attn R. Leadon
Attn R. Rose
Attn R. Stahl
Attn T. Flanagan
9775 Towne Centre Dr #3075
San Diego CA 92128-5154

Kaman Tempo
Ctr for Advncd Studies
Attn DASIAC M. Espig
PO Drawer QQ 816 State St
Santa Barbara CA 93102

Messenger & Assoc
Attn G. Messenger Suite 7-F
3111 Bel Air Dr
Las Vegas NV 89109

Mssn Rsrch Corp
Attn D. Alexander
Attn J. Tausch
Attn R. Yao
1720 Randolph Rd SE
Albuquerque NM 87106

Physics Intrntl Co
Attn Sik-Lam Wong
2700 Merced St PO Box 1538
San Leandro CA 94577

Physitron
Attn G. Grant
Attn J. Sheehy
Attn M. Christopher
Attn T. Henderson
3304 Westmill Dr
Huntsville AL 35805

Physitron Inc
Attn J. Azarewicz
Attn M. Rose
11545 W. Bernardo Ct Ste 205
San Diego CA 92128-0950

NASA Langley Research Center
Attn AMSRL-VS W. Elber
Hampton VA 23681-0001

US Army Rsrch Lab
Attn AMSRL-MA L.W. Johnson
Arsenal St
Watertown MA 02172-0001

US Army Rsrch Lab
Attn AMSRL-EP C. Thornton
Attn AMSRL-EP-P R. Hamlen
Attn AMSRL-EP-PA H. Christopher
Attn AMSRL-EP-PB S. Gilman
Attn AMSRL-EP-PD G. Guazzoni
Attn AMSRL-EP-T R. Lauttman
FT Monmouth NJ 07703-5601

US Army Rsrch Lab
Attn AMSRL-WT-PC A. Barrows
Aberdeen Proving Ground MD 21005-5066

US Army Rsrch Lab
Attn AMSRL-WT D. Eccleshall
Attn AMSRL-WT G. Klem
Attn AMSRL-WT-WG L. J. Puckett
Attn AMSRL-WT J. Frasier
Attn AMSRL-WT-NC R. Lottero
Attn AMSRL-WT-P I. May
Attn AMSRL-WT-T W. Morrison
Attn AMSRL-WT-W C. Murphy
Attn AMSRL-WT-WB W. P. D'Amico
Attn AMSRL-WT-WD A. Niiler
Attn AMSRL-CI W. H. Mermagen Sr.
Attn AMSRL-HR R. L. Keesee
Aberdeen Proving Ground MD 21005-5425

US Army Rsrch Lab
Attn AMSRL-VP R. Bill
21000 Brookpark Rd
Cleveland OH 44135-3191

Distribution

US Army Rsrch Lab
Attn AMSRL-BE COL R. Evans
Attn AMSRL-BE-A D. R. Veazey
Attn AMSRL-SL J. Wade
White Sands Missile Range NM 88002-5513

US ARDEC
Attn SMCAR-AEF-M R. B. J. Goodman

US Army Rsrch Lab
Attn AMSRL-SL-ND S. Share
Attn AMSRL-CP B. Fonoroff
Attn AMSRL-CP COL J. Correia
Attn AMSRL-CP-C D. Snider
Attn AMSRL-CP-CC J. Predham
Attn AMSRL-CP-CD A. Stewart
Attn AMSRL-CP-CD S. Karamchetty
Attn AMSRL-EP-EC A. Goldberg
Attn AMSRL-OP-SD-TL Tech Library
  (3 copies)
Attn AMSRL-OP-SD-TM Mail & Records
  Mgmt
Attn AMSRL-OP-SD-TP Tech Pub
Attn AMSRL-SL-CE A. Bevec
Attn AMSRL-SL-CE D. Manyak
Attn AMSRL-SL-CE G. W. Still
Attn AMSRL-SL-N M. Miller
Attn AMSRL-SL-NB J. Beilfuss
Attn AMSRL-SL-NB T. Flory
Attn AMSRL-SL-ND G. Merkel
Attn AMSRL-SS V. DeMonte
Attn AMSRL-SS-EE A. Lee
Attn AMSRL-SS-FC H. Brann
Attn AMSRL-SS-FD L. Ferguson
Attn AMSRL-SS-I J. Pellegrino
Attn AMSRL-SS-IB M. Patterson
Attn AMSRL-SS-IC P. Emmerman
Attn AMSRL-SS-M N. Berg
Attn AMSRL-WT-L R. Weinraub

US Army Rsrch Lab (cont'd)
Attn AMSRL-WT-N J. M. McGarrity
Attn AMSRL-WT-N W. Vault
Attn AMSRL-WT-NA R. Kehs
Attn AMSRL-WT-NB D. Davis
Attn AMSRL-WT-NB J. Gwaltney
Attn AMSRL-WT-NB M. Abe
Attn AMSRL-WT-ND J. R. Miletta
Attn AMSRL-WT-NF L. Jasper
Attn AMSRL-WT-NF T. V. H. Blomquist
Attn AMSRL-WT-NG A. J. Lelis
Attn AMSRL-WT-NG B. Lilley
Attn AMSRL-WT-NG B. McLean
Attn AMSRL-WT-NG D. Robertson
Attn AMSRL-WT-NG G. Ovrebo
Attn AMSRL-WT-NG H. Boesch
Attn AMSRL-WT-NG H. Eisen
Attn AMSRL-WT-NG J. Benedetto
Attn AMSRL-WT-NG J. Blackburn
  (25 copies)
Attn AMSRL-WT-NG J. Vanderwall
Attn AMSRL-WT-NG K. W. Be..nett
Attn AMSRL-WT-NG R. B. Reams
Attn AMSRL-WT-NG R. Moore
Attn AMSRL-WT-NG S. Murrill
Attn AMSRL-WT-NG T. Mermagen
Attn AMSRL-WT-NG T. Oldham
Attn AMSRL-WT-NG T. Taylor
Attn AMSRL-WT-NG W. Tipton
Attn AMSRL-WT-NH D. Conrad
Attn AMSRL-WT-NH G. Huttlin
Attn AMSRL-WT-NH J. Corrigan
Attn AMSRL-WT-NI A. Abou-Auf
Attn AMSRL-WT-NI C. J. Scozzie
Attn AMSRL-WT-NI J. Halpin
Attn AMSRL-WT-NI M. Bumbaugh
Attn AMSRL-WT-NW J. Ingram